SEISMIC MULTI-ATTRIBUTE ANALYSIS FOR FAULT AND FRACTURE MODELING OF AN OIL FIELD IN THE SOUTH OF IRAN

MAJID BAGHERI[1], SHAHRIYAR ASADI[2] and MEHDI TALKHABLOU[2]

[1] *Institute of Geophysics, University of Tehran, P.O. Box 14115-6466, Tehran, Iran.*
majidbagheri@ut.ac.ir
[2] *Faculty of Earth Sciences, Kharazmi University, Karaj, Iran.*

(Received March 16, 2019; revised version accepted March 10, 2020)

ABSTRACT

Bagheri, M., Asadi, S. and Talkhablou, M., 2020. Seismic multi-attribute analysis for fault and fracture modeling of an oil field in the South of Iran. *Journal of Seismic Exploration*, 29: 343-362.

Extracting geological features such as faults, and fractures using seismic data could be used to find a potential hydrocarbon reservoir and reduce the risk of production well drilling. The location and orientation of the faults are very central in investigating the efficiency of a reservoir. Also, identification of crushed zones and gas chimneys is necessary for reservoir modeling given the abundant fractures. Use of seismic attributes is significantly helpful to exploit faults and fractures from seismic data. In this study, the ant tracking method is employed for multi-attribute analysis to model fault and fractures from seismic data. The method is applied on an oil field in the South of Iran to find the medium-scale and large-to-small-scale fractures. The results obtained from the multi-attribute analysis for fracture extraction are then compared with the obtained results from FMI images, whereby a great coincidence is observed. It should be mentioned that the ability of extracted seismic attributes depends on what phenomenon is considered to detect and the quality of the original data. Totally, it could be concluded from the results that multi-attribute analysis via ant tracking is a powerful method for fault and fracture modeling.

KEY WORDS: seismic attributes, fault, fracture, FMI, reservoir.

0963-0651/20/$5.00

INTRODUCTION

Predicting the properties such as porosity, fluid saturation, permeability, from seismic data are really important for investigating a reservoir (Ba et al., 2017, 2019; Pang et al., 2019). Also, identifying the faults and fractures of a hydrocarbon reservoir is essential for reservoir management to optimize production and future developments (Nelson, 2001). But, for the reason that lots of reservoirs are complex and inhomogeneous it's hard and impossible to find a 3D fractures model just using well data (Boro et al., 2014). Therefore, seismic attributes are employed by interpreters to analyze the faults orientation and finding a 3D distribution of reservoir fractures (Chopra and Marfurt, 2007).

Seismic attributes are the most important features for seismic data interpretation. In 1990, the technology of seismic attributes is developed to use for two and three-dimensional seismic data interpretation. Bagheri et al. employed seismic attributes for facies analysis using different machine learning techniques in dissimilarity space (Bagheri et al., 2013, 2014). The basic role and ability of attributes for a reliable facies analysis and true interperetation of seismic data is irrefutble (Bagheri et al., 2017).

Lots of seimic attributes are made by a seismic wavelet created by a seismic spring, such as dynamite, with the layers boundary (reflective surfaces) of a seismic trace (Chopra and Marfurt, 2005, 2007). Simply, any linear or nonlinear change is considered on the seismic data of seismic attributes (Russell, 2004). Seismic attributes include all information obtained from seismic data, using direct methods and/or logical and empirical arguments (Taner, 2001). Basically, since 1970, countless seismic attributes have been introduced. Also, based on various purposes, different commentators have introduced new seismic attributes which are categorized from different perspectives (computational method, operational, geometric, and so on).

One of these classifications includes volumetric attributes and superficial attributes. Volumetric attributes are calculated from 3D seismic data or from attributes that have already been extracted. This happens with various mathematical algorithms, either by seismic reflected trace or by considering several of them. Calculation of these attributes in a custom and changeable window is performed as upper and lower bounds. The surface attributes can only be made on a surface to interpret a seismic horizon. Volumetric attributes are classified into several other categories which are very important for interpretation of faults and fractures of structural attributes (Fang et al., 2017).

Automatic fault detection has been done by different researchers these years (Pedersen et al., 2002; Randen et al., 2001; Hanif et al., 2014). Automatic fault-extraction technology can reduce human intervention and improve the accuracy and efficiency in fault interpretation. However, the result of automatic extraction is restricted by the parameters such as extraction sampling distance, extraction sampling threshold, extraction background threshold, deviation from a plane, connectivity constraint, minimum patch size, and patch down sampling. Extraction sampling distance sets the minimum distance between extraction seed points.

This study aims to use multi-attribute analysis for fault and fracture detection. A real data from an oil field in south of Iran is selected to test the idea and extract a reliable model of the reservoir fault and fracture distribution.

METHODOLOGY

The patent pending Ant Tracking algorithm automatically extracts fault and fractures from structural attributes (Chen and Sidney, 1997; Ngeri et al., 2015). The algorithm uses the principles from ant colony systems to extract surfaces appearing as trends in very noisy data (Chen and Liu, 2011; Ji et al., 2013; Kativar et al., 2015). Intelligent software agents ("ants") try to extract features in the attribute corresponding to the expectations of the behavior of the faults. True fault information in the attribute should fulfill these expectations and be extracted by many ants, while noise and remaining reflectors should be extracted by no ants or by only single ants. The approach is fully 3D and can take advantage of surface information in the surrounding voxels. This allows for deriving detailed information from the attribute. By writing the extracted surfaces back to a volume, we obtain what is referred to as an enhanced attribute or ant track cube (Ohmi, 2008).

This cube contains only what is likely to be true fault information. The process can be divided into four main activities: (1) seismic conditioning, (2) edge detection, (3) edge enhancement, and (4) interactive interpretation, as demonstrated in Fig. 1.

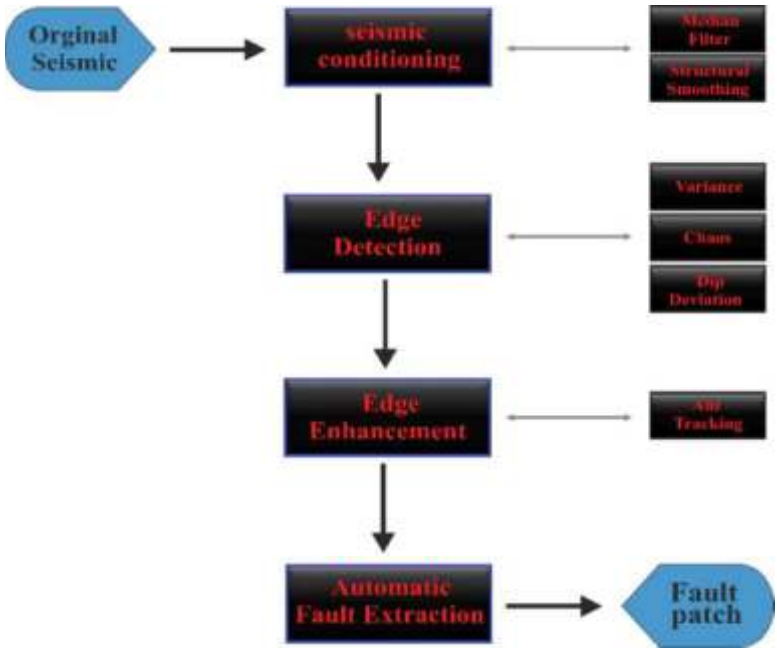

Fig 1. Ant-track workflow for creating an attribute volume and generating fault patches.

Seismic conditioning

Seismic conditioning step is used for enhancing the signal-to-noise ratio and increasing the data quality. The median filter is one of the most widely used nonlinear techniques in signal and image processing. The median filter replaces each sample in a window of a seismic trace with the median of the samples that falls within the analysis window; in so doing it rejects the outliers. The window size is typically an odd number (e.g., 3 × 3 or 5 × 5). One way to calculate the median is simply to order all of the J samples in the analysis window using an ordering index, k.

$$u_{j(1)}(t) \leq u_{j(2)}(t) \ldots \leq u_{j(k)}(t) \leq u_{j(k+1)}(t) \ldots \leq u_{j(J)}(t) \quad . \quad (1)$$

The median is then given by:

$$u_{median}(t) = u_{j\left(k=\frac{[J+1]}{2}\right)}(t) \quad . \quad (2)$$

Structural smoothing of the input signal is guided by the local structure to enhance the continuity of the seismic reflectors (Randen, 2001). Principal component dip and azimuth computation are used to determine the local structure. Gaussian smoothing is then applied parallel to the orientation of this structure.

Edge detection

The spatial discontinuities in seismic images can be enhanced using any of the edge detection methods (variance, chaos, dip deviation). Another popular measure of waveform similarity is the variance. As implemented, the variance estimate of coherence is identical to the semblance estimate discussed above. Modifying the mathematical formula of variance, var(t,p,q), to be computed along samples lying on a dipping reflector, we write:

$$\mathrm{Var}(t,p,q) = \frac{1}{J}\sum_{j=1}^{J}\left[u_j\left(t - px_j - qy_j\right) - u(t,p,q)\right]^2 \quad , \tag{3}$$

where the mean, <u(t,p,q)>, is defined as:

$$u(t,p,q) = \frac{1}{J}\sum_{j=1}^{J} u_j\left(t - px_j - qy_j\right) \quad . \tag{4}$$

Note here that <u> is calculated for each plane parallel to the reflector with the analysis window. Although Equations 3 and 4 provide the mathematical formula of variance, most statisticians employ a far more efficient (and mathematically equivalent) computation for:

$$\mathrm{Var}(t,p,q) = \frac{1}{J}\sum_{j=1}^{J}\left[u\left(t - px_j - qy_j, x_j, y_j\right)\right]^2 - \left[\frac{1}{J}\sum_{j=1}^{J} u\left(t - px_j - qy_j, x_j, y_j\right)\right]^2 \quad . \tag{5}$$

Dip deviation attributes can highlight the faults with displacements having offsets significantly less than the width of the seismic wavelet. Out of dip categories: in-line dip, cross-line dip and polar dip, cross-line dip is considered to be the most important dip because of its coherency with the direction of faults.

Chaos attribute is defined as measure of the “lack of organization” in the dip and azimuth estimation method. In other words, chaos attribute can detect chaotic textures within seismic data, which can directly highlight the positions of reflector disruption. Accordingly, chaos attributes can be used to detect a fault.

Edge enhancement

In nature, ants, while seemingly simple, use swarm intelligence to accomplish complex tasks such as finding food and building nests. When searching for food, ants use pheromone trails to direct other colony members to food they have found. Through this process, the ants find the most efficient path from the nest to the food. Similarly, by populating a preprocessed 3D seismic volume with computer agents coded to follow discontinuities, swarm intelligence is used to identify, track, and sharpen faults. When ants move from the source point to destination point, they leave a chemical called pheromone to mark these paths. This helps the following ants to find the way of their team members as they detect pheromone and choose, in probability, paths with a greater concentration of pheromone. The ants are driven by a probability rule to choose their solution to the problem, known as a tour. An ant will move from node i to node j with the probability:

$$p_{ij}^{k}(t) = \frac{[\tau_{ij}(t)]^{a}[\eta_{ij}]^{\beta}}{\sum[\tau_{ij}(t)]^{a}[\eta_{ij}]^{\beta}} \ , \eta_{ij} = \frac{1}{d_{ij}} \quad , \tag{6}$$

η_{ij} is the amount of pheromone on edge i, j, a is a parameter to control the influence of τ_{ij}, η_{ij} represents the desirability of edge (i, j), and β is a parameter to control the influence of η_{ij}.

During the movement of the ant on the path, the amount of pheromone is updated according to the equation:

$$\tau_{ij}(t+1) = \rho.\ \tau_{ij}(t) + \sum \Delta\tau_{ij}^{k}(t) \quad , \tag{7}$$

ρ is the evaporation rate ($0 \leq \rho \leq 1$), k *shows* the number of ants, and $\Delta\tau_{ij}^{k}$ denotes pheromone quantity laid on edge (i, j) by the *k*-th ant.

APPLICATION

The seismic data were selected from the Balal oil field located in the Persian Gulf, near the Iranian and Qatar border, 50 miles away from the southwest of Lavan Island and 25 miles from southeast of the South Pars gas field. The most important structural elements that control the tectonic state of the area are as follows (Stöcklin, 1968):

- North-south constructional processes, including available bulge and faults on the stone foundation, known as the ancient process of Arabic plate.

- Faults and construction projects with a north western-southeastern pattern. This pattern is the main direction of the major faults and the suture zone with the two-sided Arabic plate.
- Structures arising from the bulging Precambrian salts, which is a young tectonic phenomenon.

Seismic conditioning

In accordance with the analytical method mentioned in the last chapter, to remove the random noises and enhance the signal-to-noise ratio, median and structural smoothing filters are compared. In both filters, the averaging algorithm is used to eliminate noise. We applied both filters on the seismic data with the results were obtained according to the imaging.

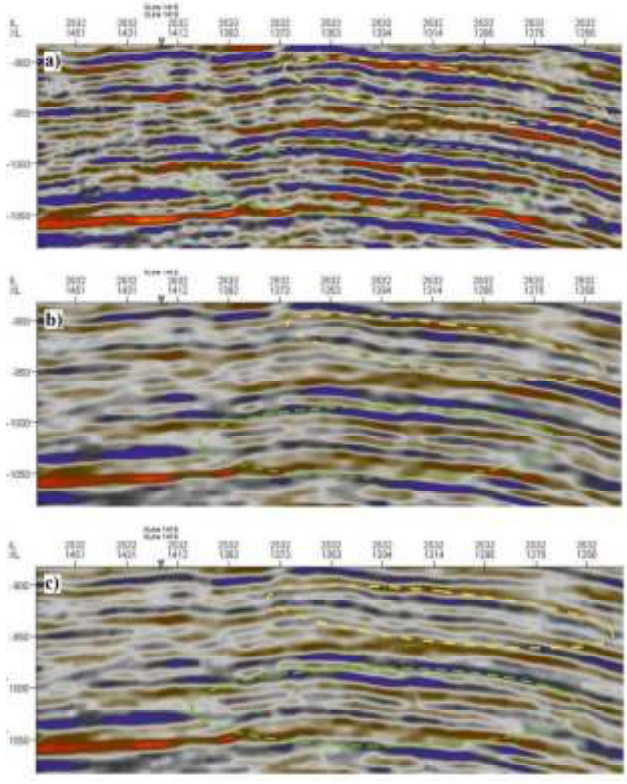

Fig 2. a) Seismic data before filtering. b) The data after applying median filter. c) The data after structural smoothing.

According to Fig. 2, in the green and yellow areas, it is observed that the median filter provides better result for random noise attenuation and increasing the continuity of seismic events in comparison with structural smoothing.

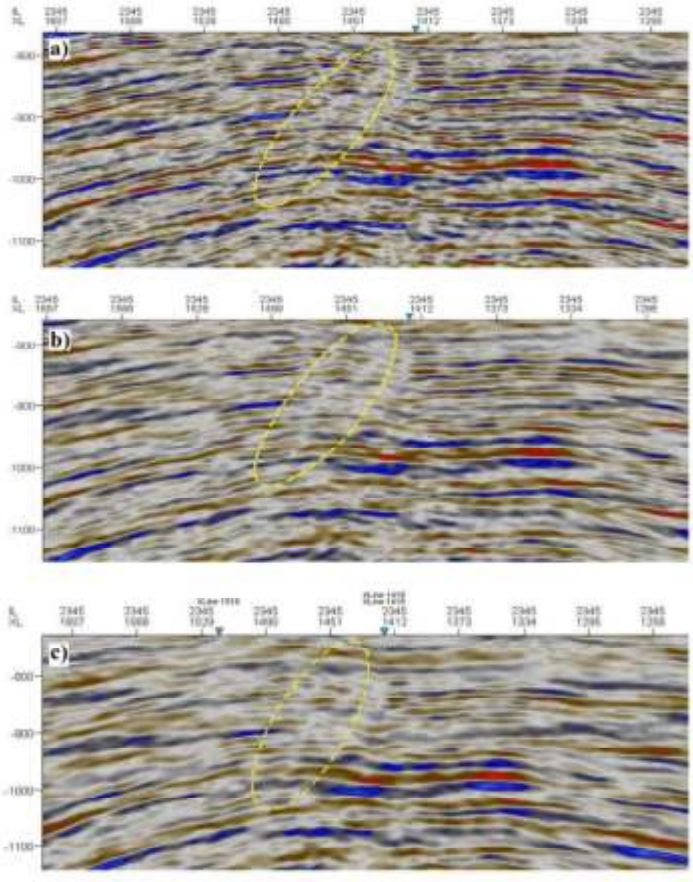

Fig 3. a) Seismic data after median filtering with voxel radius of 1, b) Seismic data after applying median filter with voxel radius of 3, c) seismic data after median filtering with voxel radius of 5.

As pointed out in the theoretical part of the method, the exploration of attributes parameters can extract significant results from seismic data. We can apply the Median filter attributes with different parameters on the

seismic data. For this purpose, the number of selected samples (voxel) to run the median filter is important. This is important also that by considering that this filter can be applied in radials from 1 to 5 voxels (odd numbers) on how many samples this filter can be applied. To achieve this goal, this filter was applied to the seismic data with different parameters. The obtained results are as follows:

According to Fig. 3a, the median filter attributes were applied with the parameters including inline radius: 1 xline radius: 1, depth radius:1. Based on the obtained results, this filter with the chosen parameter, ie, the radius of one voxel, has not provided a satisfactory result. Specifically, this filter has acted very poorly with the parameter specified in the removal of noises, the edge detection, and the reinforcement of the reflectors.

In Fig. 3b, the median filter attributes were applied with the parameters such as 3: Inline radius 3: xline radius: 3 depth radius. As observed in the image, the noise has been removed better than in the 6-6 image. Furthermore, the reflectors are reinforced and its fault line, as indicated by dark yellow lines, and you can see it better.

In Fig. 3c, we applied the median filter attributes with the parameters including 5: Inline radius 5: xline radius 5: depth radius. According to the image, this filter with a number of samples in the 5-voxel radius has effectively eliminated the noise. However, regarding the indicated location in the image, its fault line and some reflectors or seismic horizons have also been removed, suggesting weakening of the amplitude.

In general, at the end of this step for the median filter, consideration of 3 voxel radius is appropriate for applying the filter. If a number beyond 3 is to be considered, it leads to loss of reflectors. Further, the structural phenomena such as faults are also removed. It can be concluded that for applying the median filter, the results obtained in Fig. 9 are the best possible mode.

Edge detection

For this purpose, as already expressed in the study method, we use the variance, chaos, and dip deviation attributes. In this stage, we apply all of the three above-mentioned attributes from the median filter. Then, the results should be checked and analyzed Note that at this stage, application of the attributes on the time slice window is analyzed, as these attributes show themselves better in the time slice.

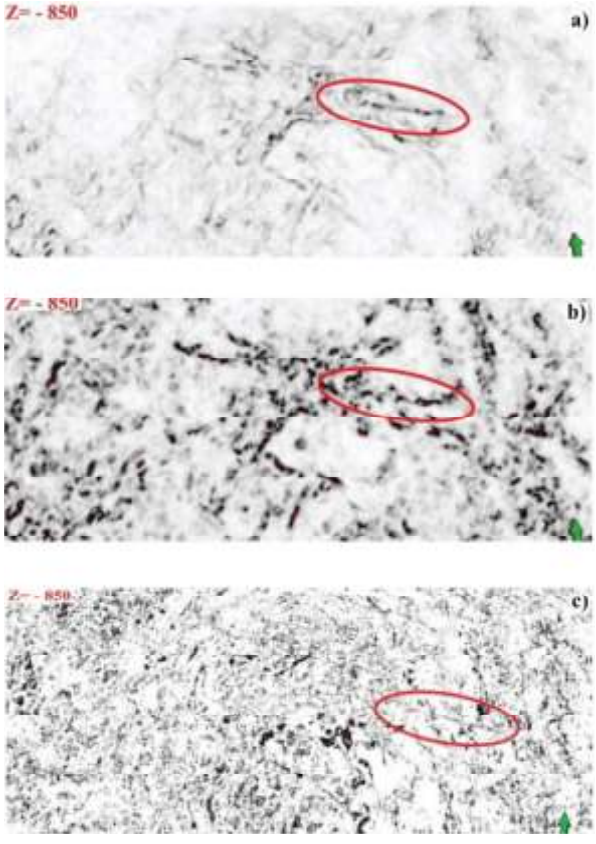

Fig 4. a) The variance attribute of the data in time slice z = -850. b) The chaos attribute of the data in time slice z = -850. c) The Dip deviation attribute in time slice z = -850.

According to Fig 4a, the variance attributes have been applied on the seismic data. Also, as observed by the red circle, the results show that the variance attributes have revealed the discontinuity region well, and the fault line is clearly seen.

Fig. 4b demonstrates the ability of chaos attributes in detecting the irregularities of the zones and disorganization of the reflectors. However, it is not possible to determine the location of the fault by the results obtained from these attributes. According to the area marked with the red circle, these

attributes have been able to represent disorganization of the seismic horizons. Nevertheless, it cannot be claimed that the location of the fault line has been determined. In Fig. 4c, by applying the dip deviation attributes, the variation and slope deviation of amplitude have been measured, whereby the discontinuity region is revealed. Given the location marked with the red circle, these attributes have not been able to detect the location of the fault. Also, according to the following probability, these attributes makes result for very clear discontinuities.

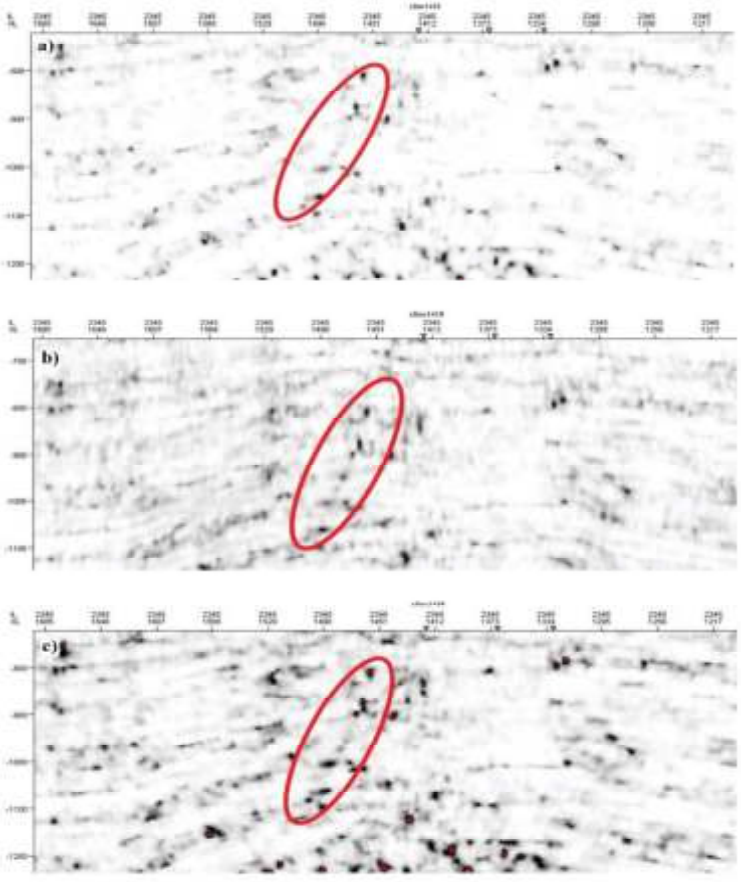

Fig 5. a) Variance attribute with inline range: 2, crossline range: 2, vertical smoothing: 13 parameters, b) variance attribute with inline range: 3, crossline range: 3, vertical smoothing: 13 parameters, c) variance attribute with inline range: 4, crossline range: 4, vertical smoothing: 13 parameters.

The results obtained from applying the above attributes suggest that the variance attributes have been better than the two chaos and dip deviation attributes, providing a better view for the interpretation of faults and fractures. Applying attributes with different parameters will alter the quality of obtained results, which can paradoxically improve the quality of the results or reduce their quality. As stated earlier, the variance attributes have been superior than the other two attributes in revealing the fault. As such, it is possible to obtain other results by changing their parameters. For the variance attributes, the number of reflected seismic samples is very important for measuring the variance. It is important that the number of samples is 4, 9, or 16. Here, we apply the variance attributes with different parameters. The samples have been selected in different directions including inline, cross-line, and vertical. In the directions of inline and crossline, a number of seismic samples have been selected for variance.

However, in the vertical direction, a period is considered for selecting the amplitude chosen from the average reflected seismic data of the studied field. This period in the standard state is 15 milliseconds, but for the seismic data of the Balal field, it has been measured as 13 milliseconds.

The variance attribute was applied with the parameters Inline range: 2 crossline range: 2 vertical smoothing: 13 ms (see Fig. 5a). As observed in Fig. 5a, the effects of discontinuity are seen in the specified area with the red circle, but the location of fault line is not seen well and it does not offer an appropriate resolution.

According to Fig. 5b, we applied the variance attribute with the parameters inline range: 3 crossline range: 3 vertical smoothing: 13 ms. It is obvious that better result than the Fig. 5a is resulted. As marked in the red circle, we can see the fault line, though its resolution is low.

In Fig. 5c, the location marked with the red circle represents the result obtained from applying variance with the parameters such as inline range: 4 cross line range: 4 vertical smoothing: 13 ms. The disorganization of the seismic horizons has been specified and the discontinuities are shown, but its fault line is not seen. As the number of samples for achieving variance is high, the numbers of the variance are closer to each other and the discontinuities are removed.

By applying the variance attributes with different parameters, it was found that the variance attributes with the parameters such as inline range: 4 cross line range: 4 vertical smoothing: 13 ms show the most favorable response compared to the other applied parameters for detecting fault and fractures lines.

Edge enhancement

The results from obtained edge detection were used along with the ant tracking attributes for this stage. In this chapter, its analysis method was explained. Given that our goal is to extract the faults, we determined specific parameters for the ant tracking attributes, according to Table 1 and then applied it on the seismic data.

According to Figs. 6a, b, and c, the ant tracking attributes are shown with the parameter reported in Table 1 and was applied like variance, chaos, and dip deviation attributes.

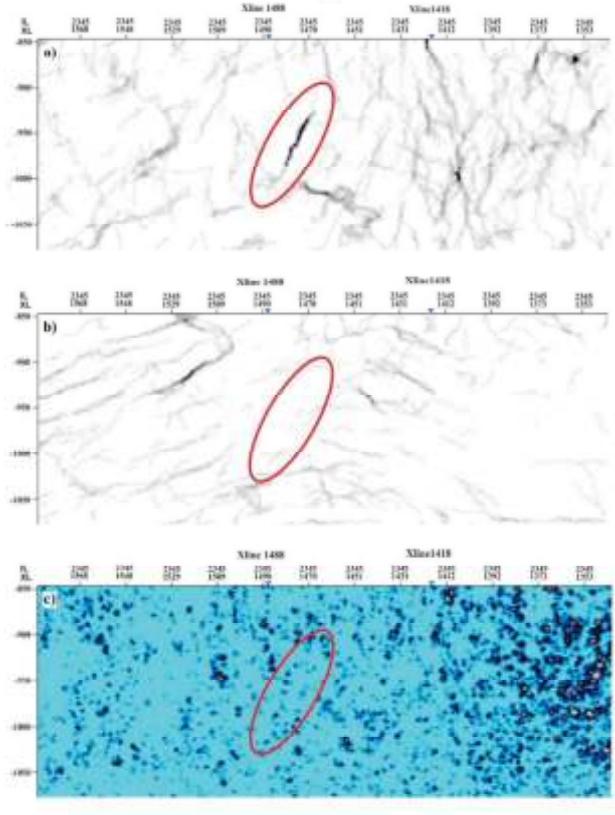

Fig 6. a) Application of ant tracking on the variance attribute managing to identify the major fault in the red circle area, b) Major faults not recognized after applying ant tracking attributes on the chaos attribute, c) Using ant tracking attributes on the dip deviation attribute, the major fault has not been identified.

Table 1. The ant tracking parameters used in this study.

Initial Ant Boundary	Ant Track Deviation	Ant Step Size	Illegal Steps Allowed	Legal Steps Required	Stop Criteria
5	2	3	2	2	10

As seen in the above images and in the specified location, application of the ant tracking attributes derived from the variance attributes gives the best answer. Note that applying the ant tracking attributes from the two other attributes does not seem reasonable. It is because the ant tracking attributes follow linear discontinuities; It can deviate only 15° from its path, while an attribute like the chaos can measure the amount of irregularities. If these attributes are applied from the chaos attributes, it cannot follow the linear discontinuities well, and will yield a wrong answer. It is seen in the images that the tracking from chaos and dip deviation attributes has not been able to reveal even the exact location of the fault.

FAULT AND FRACTURE EXTRACTION AND INTERPRETATION

Each fractured fragment is extracted from analysis of multi-indicative seismic data with different areas, slopes, and lengths compared to each other. Using the histogram filter, we filtered these pages in terms of area and removed small fractures from this data. It was observed that the slope and stretching large fractures are according to the available tectonic and faults in the field.

The right-hand side of Fig. 7 displays the dip and the azimuth of the fault as well as the fractures derived from the multi-attribute analysis. On the other hand, the left-hand side of Fig. 7 reveals the major faults in the field, which are marked with green and yellow lines. All of them are steep and have extended to northern-southern and north western-south eastern sides. The results obtained from multi-attribute analysis are consistent with actual data. The two factors including regional tectonic and the existence of salt diapirs play an essential role in the formation of faults and fractures in this field. The motion of the Arabic plate in the direction of the north-eastern and its pressure to the Iranian sight have caused the creation of Zagros Mountains and the creation of faults along the North West-South-East and Northern-Southern in the Persian Gulf. Salt diapiris has also made the Balal field in form of an anticline, resulting development of fractures.

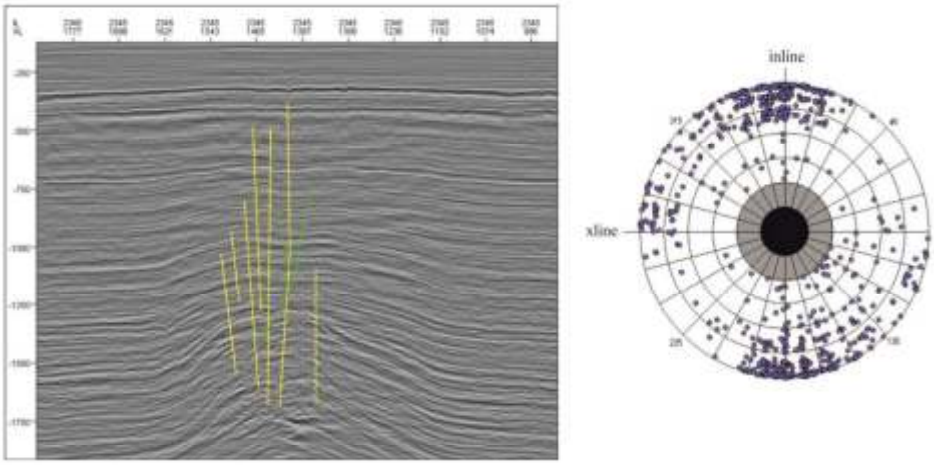

Fig 7. Left: Major faults in the studied field area. Right: Dip and the azimuth of the faults and large-scale fractures resulting using attributes analysis.

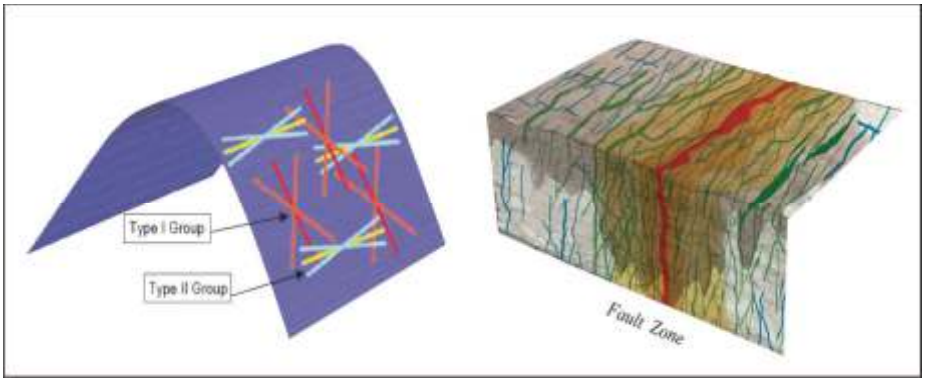

Fig. 8. Orientation of fractures in the fault zone and folding zone of the Balal oil field.

According to Fig. 8, the fractures created in the fault zone usually make a form parallel to the fault line, where the fractures resulting from wrinkling are divided into parallel and cross-sectional groups with a wrinkled edge and in accordance with the above figure.. The results obtained (see Fig. 9) from the analysis of multi-attribute seismic data from the Balal field prove the existence of such structures and fractures.

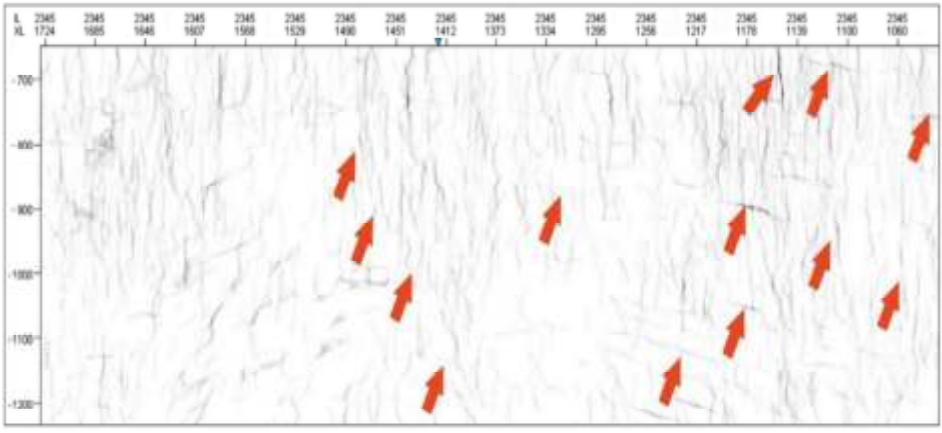

Fig. 9. Fault and fracture orientation resulted using attribute analysis in the studied area.

FMI IMAGES

The FMI images are as a powerful tool for studying fractures in wells. The image graph is a pseudo-image with high resolution from the wall of well. These graphs provide important information about the orientation, depth, and type of natural fractures. Fracture analysis is one of the most important goals in scanning FMI images.

These images are used to categorize and accurately determine fracture characteristics, including slope, azimuth, and to estimate fracture properties such as opening. The analysis of fractures in the BL-12P well can be summarized as follows:

Based on Fig. 10, most of the fractures have a slope greater than 78 degrees or have a vertical position. These fractures extend in northern-southern and northwest-southeast directions, while a limited number of them are in the northeast-south west (N55E) direction. The direction of most of these fractures depends on two factors of wrinkling due to rise of the salt diapiris and the presence of multiple and steep faults with the fractures developed in their parallel.

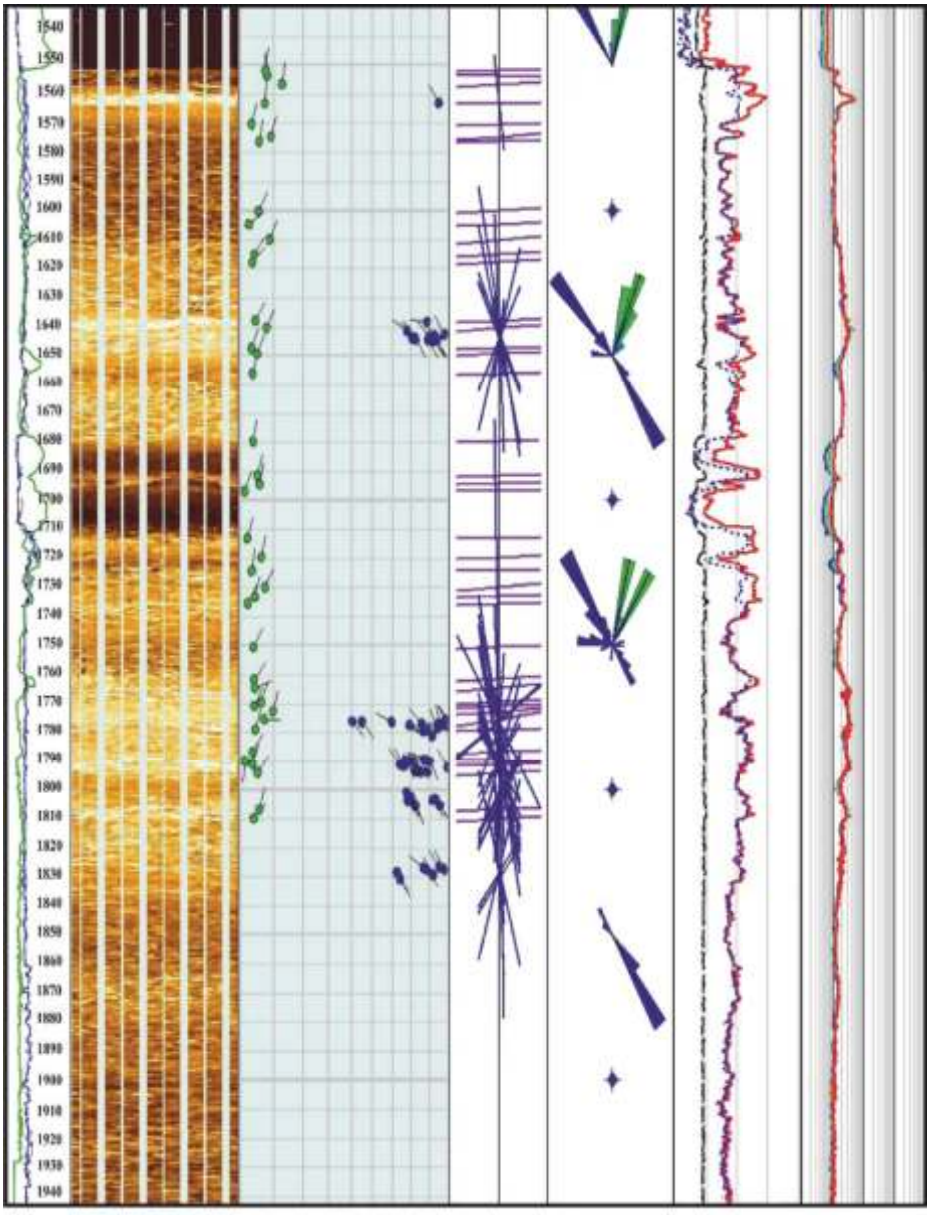

Fig. 10. Fracture analysis results in the well BL-12P, most of the conductive fractures seem to be developed in the middle part of Khatiyah formation.

These images are used to categorize and accurately determine fracture characteristics, including slope, azimuth, and to estimate fracture properties such as opening The analysis of fractures in the BL-12P well can be summarized as follows:

Based on Fig. 10, most of the fractures have a slope greater than 78 degrees or have a vertical position. These fractures extend in northern-southern and northwest-southeast directions, while a limited number of them are in the northeast-south west (N55E) direction. The direction of most of these fractures depends on two factors of wrinkling due to rise of the salt diapiris and the presence of multiple and steep faults with the fractures developed in their parallel.

CONCLUSION

Modeling the faults and fractures of an oil reservoir is necessary for finding the best location of a production well. For this aim, in this study we employed seismic multi-attribute analysis for fault and fracture detection. A real data from an oil field in south of Iran was selected for modeling fault and fracture distribution. Based on the presence of salt diapirism, many faults (with near vertical slopes) and fractures with different characteristics have been made in the field.

For investigating the idea, the first step is improving the quality of seismic data using median filter and structural smoothing. The results of data quality improvement indicated that the median filter is more powerful compared to structural smoothing with the following parameters; Inline radius: 3, depth radius: 13, and xline radius: 3. In the second step, edge detection or discontinuity, three attributes including variance, chaos, and dip deviation were used. Having applied and analyzed the attributes, it was observed that variance attributes with the parameters of depth radius: 3, inline range: 3, and cross line range: 13, constituted the best for edge and discontinuity detection. In the third step, the ant tracking attributes were employed for edge enhancement.

After these steps, for extracting different scales of fractures, the attributes with the parameters specified in Table 1 were applied. The final results of multi-attribute analysis for fracture extraction were compared with the results obtained from FMI images, whereby a great coincidence was observed.

We converted the obtained discontinuity lines into fault and fracture fragments and removed small plates showing small fractures by histogram filtering. The existence of large faults and great fractures with the northern

southern and northwestern-southeastern direction suggests that the results of multi-attribute analysis are consistent with the tectonic of the region. Finally, from the results it could be concluded that multi-attribute analysis is powerful for extracting an accurate model of fractures and faults of the reservoir.

ACKNOWLEDGEMENT

The authors gratefully acknowledge the Institute of Geophysics, University of Tehran and the Kharazmi University for supporting this research.

REFERENCES

Ba, J., Ma, R.P., Carcione, J.M. and Picotti, S., 2019. Ultrasonic wave attenuation dependence on saturation in tight oil siltstones. Journal of Petroleum Science and Engineering, 179:1114-1122.

Ba, J., Xu, W.H., Fu, L.Y., Carcione, J.M. and Zhang, L., 2017. Rock anelasticity due to patchy-saturation and fabric heterogeneity: A double double-porosity model of wave propagation. J. Geophys. Res. - Solid Earth, 122: 1949-1976.

Bagheri, M., Riahi, M.A. and Hashemi, H., 2013. Reservoir lithofacies analysis using 3D seismic data in dissimilarity space. J. Geophys. Engineer., 10: 035006.

Bagheri, M. and Riahi, M.A., 2014. Seismic facies analysis from well logs based on supervised classification scheme with different machine learning techniques. Arab J. Geosci. DOI; 10.1007/s12517-014-1691.

Bagheri, M. and Riahi, M.A., 2017. Modeling the facies of reservoir using seismic data with missing attributes by dissimilarity based classification. J. Earth Sci., 28: 703-708.

Boro, H., Rosero, E. and Bertotti, G, 2014. Fracture-network analysis of the Latemar Platform (northern Italy): Integrating outcrop studies to constrain the hydraulic properties of fractures in reservoir models. Petrol. Geosci., 20: 79-92.

Chen, E. and Liu, X., 2011. Multi-colony ant algorithm. In ant colony optimization-methods and applications. Intech, Croatia:3-12.

Chen, O. and Sidney, S., 1997. Seismic attribute technology for reservoir forecasting and monitoring. The Leading Edge, 16: 445-448.

Chopra, S. and Marfurt, K.J., 2005. Seismic attribute: A historical perspective. Geophysics, 70(5): SO3-SO28.

Chopra, S. and Marfurt, K.J., 2007. Seismic Attributes for Prospect Identification and Reservoir Characterization. SEG, Tulsa, OK.

Chopra, S. Marfurt, K.J., 2007. Volumetric curvature attributes for fault/fracture characterization. First Break, 25: 35-46.

Fang, J., Zhou, F. and Tang, Z., 2017. Discrete fracture network modelling in a naturally fractured carbonate reservoir in the Jingbei oil field China. Energies, 10: 183.

Hanif, S., Tariq, A., Ahmed, A.I. and Hanif, A, 2014. Ant tracking algorithm for surface discontinuity extraction-faults detection. Robotics and Emerging Allied Technologies in Engineering (iCREATE), IEEE: 235-238.

Ji, J., Liu, Z., Zhang, A., Yang, C. and Liu, C., 2013. HAM-FMD: mining functional modules in protein–protein interaction networks using ant colony optimization and multi-agent evolution. Neurocomputing, 121: 453-469.

Kativar, S., Ibraheem, N. and Ansari, A.Q., 2015. Ant colony optimization: a tutorial review. MR Internat. J. Engineer. Technol., 7(2): 35-41.

Nelson, R.A., 2001. Geologic Analysis of Naturally Fractured Reservoirs, 2nd Ed. Gulf Professional Publishing, Houston.

Ngeri, A.P., Tamunobereton-ari, I. and Amakiri, A.R.C., 2015. Ant-tracker attributes: an effective approach to enhancing fault identification and interpretation. J. VLSI Sign. Process., 5: 67-73.

Ohmi, K., Sapkota, A. and Pandav, S.P., 2008. Applicability of ant colony optimization in particle tracking velocimetry. Proc. 14th Internat. Symp. Applicat. Laser Techn. Fluid Mechan., Lisbon.

Pang, M.Q., Ba, J., Carcione, J.M., Picotti, S., Zhou, J. and Jiang, R., 2019. Estimation of porosity and fluid saturation in carbonates from rock-physics templates based on seismic Q. Geophysics, 84(6): 1-51.

Pedersen, S.I., Randen, T., Sønneland, L. and Steen, Ø., 2002. Automatic fault extraction using artificial ants. Expanded Abstr., 72nd Ann. Internat. SEG Mtg., Salt Lake City: 512-515.

Randen, T., Pedersen, S.I. and Sønneland, L., 2001. Automatic extraction of fault surfaces from three-dimensional seismic data. Expanded Abstr., 71st Ann. Internat. SEG Mtg., San Antonio: 551-554.

Russell, B.H., 2004. The application of multivariate statistics and neural networks to the prediction of reservoir parameters using seismic attributes. PH.D. thesis, University of Calgary, Alberta.

Stöcklin, J., 1968, Salt deposits of the Middle East. GSA - Special paper, 88: 157-181.

Stöcklin, J., 1968, Structural history and tectonics of Iran: a review. AAPG Bull., 52: 1229-1258.

Taner, M.T., 2001. Seismic attributes. CSEG Recorder, 26(7): 48-56.